AIMS Mathematics, 11(7): 22114–22132.
DOI: 10.3934/math.2026895
Received: 20 May 2026
Revised: 03 July 2026
Accepted: 10 July 2026
Published: 24 July 2026

https://www.aimspress.com/journal/Math

Research article

Analytical study of degree-based graphical invariants in subdivided hexagonal cage networks

Muhammad Abdullah[1], **Muhammad Usman Ghani**[2,*], **Hanen Karamti**[3] **and Syed Ajaz K. Kirmani**[4]

[1] Department of Mathematics, Government College University, Lahore, Pakistan
[2] Institute of Mathematics, Khawaja Fareed University of Engineering & Information Technology, Abu Dhabi Road, 64200, Rahim Yar Khan, Pakistan
[3] Department of Computer Sciences, College of Computer and Information Sciences, Princess Nourah bint Abdulrahman University, P.O. Box 84428, Riyadh 11671, Saudi Arabia
[4] Department of Electrical Engineering, College of Engineering, Qassim University, Buraydah, Saudi Arabia

* **Correspondence:** Email: usmanghani85a@gmail.com.

Abstract: Graphical invariants and degree-based topological indices are important tools in graph theory, network science, and mathematical modeling for characterizing the structural properties of complex graph families. In this paper, we investigated subdivided hexagonal cage networks and derived exact analytical expressions for several important graphical invariants, including the general Randić index, the first Zagreb index, the second Zagreb index, the third Zagreb index, the atom-bond connectivity index, and the hyper-Zagreb index. By employing graph-theoretical techniques together with edge partition methods, explicit closed-form formulas were obtained in terms of the subdivision parameter of the underlying network. The derived results demonstrate the impact of subdivision operations on the structural behavior, branching characteristics, and quantitative complexity of the considered networks. Moreover, these graphical invariants provide useful insights into the structural characteristics, connectivity patterns, and complexity of the considered subdivision networks. The presented framework enriches the study of graphical invariants for nanostructures and complex graph and network models, while also contributing to applications in mathematical chemistry, materials science, and graph-based network analysis.

Keywords: graphical invariants; chemical graph theory; topological indices; degree-based indices; general Randić index; Zagreb indices; atom–bond connectivity index; hyper-Zagreb index; subdivided hexagonal cage networks
Mathematics Subject Classification: 05C09, 05C12, 05C90

1. Introduction

Graph theory, with numerous applications in various scientific fields, especially chemistry, is a rapidly expanding area. It is essential for the study of molecular (structural) graphs, which are often represented as hydrogen-suppressed graphs [1, 2]. The study and representation of chemical structures using graph-theoretical methods is a key component of cheminformatics, an interdisciplinary field that integrates information science, mathematics, and chemistry [3].

A graph is a structure consisting of vertices connected by edges, where the vertices represent discrete points and the edges represent connections between them. The concept of distance-based entropy extends classical graph-theoretic analysis by incorporating the shortest-path distances among vertices to quantify the structural complexity and information distribution within a network [4, 5]. A chemical graph is a mathematical representation of a molecule in which vertices correspond to atoms and edges correspond to chemical bonds [6]. Research in chemical graph theory has important real-world applications, including toxicity prediction, drug development, and materials science [7]. By studying the complex relationship between molecular topology and molecular properties, researchers can design more effective drugs and advanced materials while accurately predicting their behavior in various scenarios. These investigations provide profound insights into the fundamentals and practical applications of chemical graph theory [8].

The study of topological indices in relation to molecular structures benefits multiple fields, including materials science and drug design. These indices offer significant insights into molecular properties and serve as effective tools for designing safer and more efficient drugs [9]. Such analyses improve our understanding of molecular behavior [10, 11] and its applications by elucidating the relationship between molecular topology and intrinsic characteristics; see Figure 1.

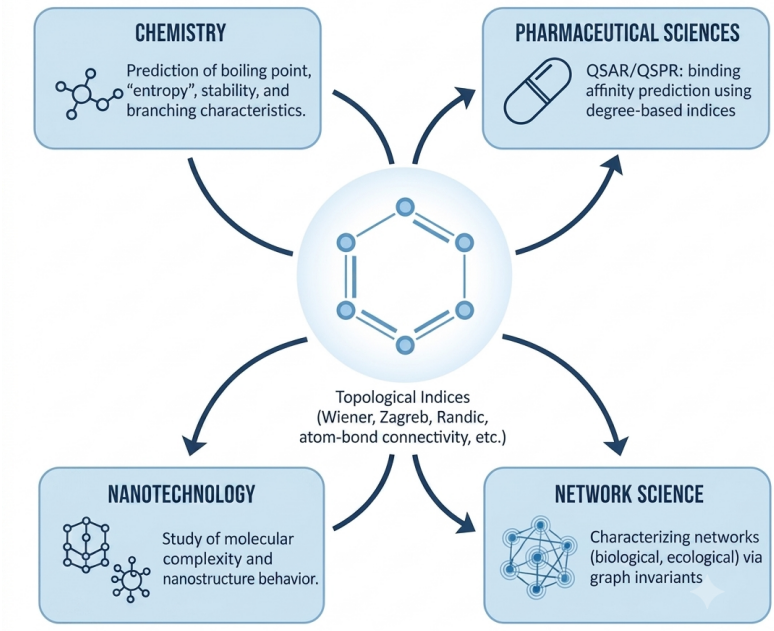

Figure 1. Applications of topological indices in science.

Topological indices allow for the analysis and prediction of physical properties, chemical reactivity,

and even some biological activities of molecules [12, 13]. Thus, they provide an efficient approach that can reduce time and cost associated with extensive laboratory experiments [14, 15].

Harry Wiener first studied the boiling points of thirty-seven paraffins, ranging from C_4H_{10} to C_8H_{18}. He applied the least-squares method to analyze these compounds [16, 17] and observed that their properties depend not only on the chemical composition but also on the shape, size, branching, and other factors [18, 19]. Numerous studies on topological indices [20, 21], including degree-based, distance-based [22, 23], atom-bond connectivity, and geometric-arithmetic indices, have been conducted to analyze chemical molecules [24, 25].

Randić [26] introduced a degree-based topological index known as the Randić index, $R_{1/2}(G)$, which exhibits good correlation with many physical and biochemical properties: The ordinary Randić index of a graph G is defined as

$$R_{-\frac{1}{2}}(G) = \sum_{uv\in E(G)} \frac{1}{\sqrt{d(u)d(v)}}. \tag{1.1}$$

The generalized Randić index (also known as the connectivity index) of a graph G is defined by

$$R_\alpha(G) = \sum_{uv\in E(G)} [d(u)d(v)]^\alpha, \tag{1.2}$$

where α is a real number. In particular, $R_{-\frac{1}{2}}(G)$ is the ordinary Randić index [27].

Another well-known topological index is the first Zagreb index, denoted by $M_1(G)$, introduced by Gutman and Trinajstić:

$$M_1(G) = \sum_{uv\in E(G)} [d(u) + d(v)]. \tag{1.3}$$

Estrada et al. [28] introduced the atom–bond connectivity (ABC) index:

$$ABC(G) = \sum_{uv\in E(G)} \sqrt{\frac{d(u) + d(v) - 2}{d(u)d(v)}}. \tag{1.4}$$

The geometric–arithmetic (GA) index is another important degree-based topological index [29, 30]:

$$GA(G) = \sum_{uv\in E(G)} \frac{2\sqrt{d(u)d(v)}}{d(u) + d(v)}. \tag{1.5}$$

Shi et al. [31] conducted an in-depth examination of flabellum graphs using different degree-based topological indices such as the Randić index, atom-bond connectivity index, geometric-arithmetic index, and Zagreb indices. Lal et al. [32] used the M-polynomial and NM-polynomial techniques to compute various degree-based and neighborhood-degree-sum-based topological indices of complex crystal structures in emerging nanomaterials of lead sulfide (PbS). Sharma et al. [33] computed the second leap hyper-Zagreb coindex and polynomial for certain classes of benzenoid structures, including zigzag benzenoid, rhombic benzenoid, multiple segment linear hexagon chains, and hammer-like benzenoid. Lal et al. [34] employed the NMpolynomial technique to calculate various neighborhood-degree-sum-based topological indices and graph-based entropies for carbon nanotube

Y-junction graphs. Sharma et al. [35] investigated the antiviral drugs oseltamivir and zanamivir by calculating their topological indices and examining their metric and edge metric resolvability, providing insights into the structural and functional properties of these compounds. Nitrogen's isolated hexagon atomic structure demonstrates a special hexagonal configuration where nitrogen atoms form discrete hexagonal rings that are isolated from one another, indicating a stable and symmetric molecular configuration as in Figure 2.

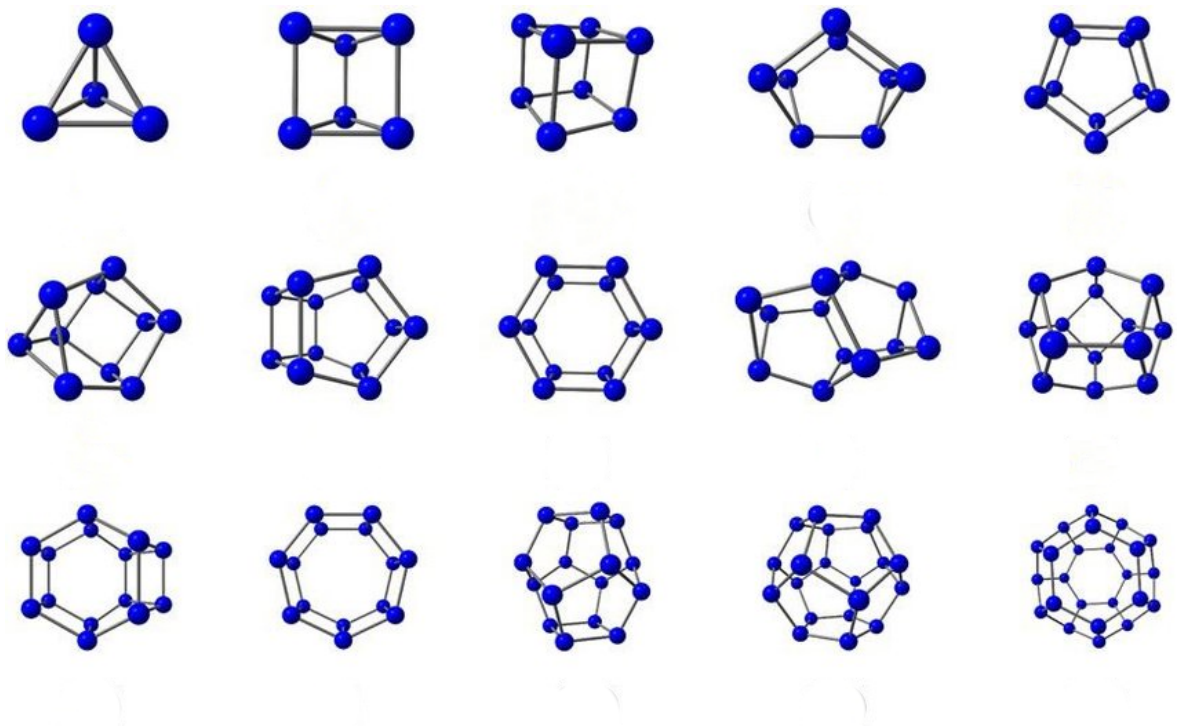

Figure 2. The atomic structure of nitrogen with isolated hexagons.

Although degree-based topological indices originated in chemical graph theory [36], they are now extensively investigated for a wide range of generalized graph families and complex networks. In this work, the subdivided hexagonal cage network is studied as a mathematical graph rather than a classical molecular graph. Our objective is to derive exact analytical expressions for several degree-based graph invariants, thereby contributing to the theory of graph invariants and the structural analysis of subdivision networks.

2. Main results

In this article, we extend the concept of the hexagonal cage network $HX(C_p^q)$ by applying the process of edge subdivision, resulting in the subdivided graph denoted by $G = S(HX(C_p^q))$ of order p with q copies.

We calculate various topological indices (TIs) for these subdivided networks, including the general Randić index, the first, second, and third Zagreb indices, the geometric index, the atom-bond connectivity (ABC) index, and the hyper-Zagreb index. Furthermore, we provide graphical illustrations in both 2D and 3D for all TIs to facilitate comparison across the family of subdivided hexagonal cage

networks $S(HX(C_p^q))$. Nitrogen nanotube graphs with wall structures made up of sequences of three or four hexagonal faces can be used to describe tubular nitrogen clusters with neighboring hexagons from a graph-theoretical standpoint. These nanotube networks' terminal ends have caps that represent subgraphs made up of one or three vertices in the three-hexagon configuration, and two or four vertices in the four-hexagon configuration, as shown in Figure 3.

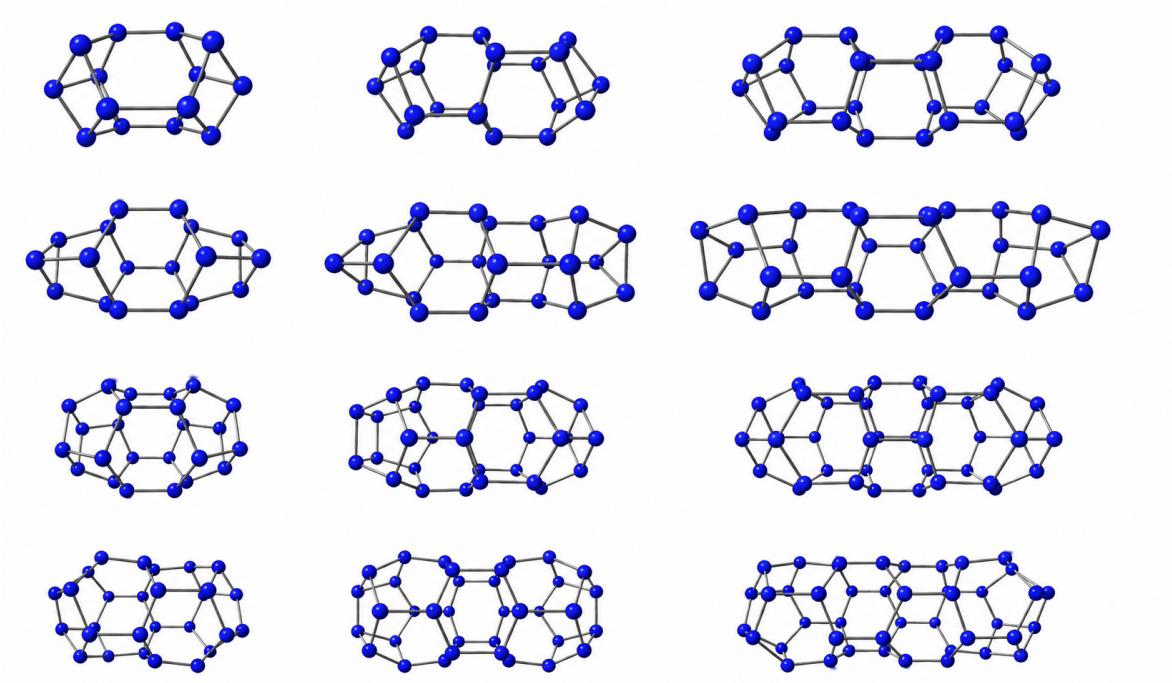

Figure 3. Hexagon configuration.

2.1. Hexagonal cage network $S(HXC_p^q)$: construction algorithm

The construction algorithm for the hexagonal cage network, denoted as $S(HXC_p^q)$, is described as follows:

Step 1: Begin with a q-dimensional hexagonal network, denoted by $HX(q)$.

Step 2: Attach the boundary vertices of $HX(q)$ to the corresponding boundary vertices of its mirror copy. This process generates a cage network composed of two copies of $HX(q)$, joined along their edges to form a cohesive structure, see Figure 4.

Step 3: To incorporate a third copy of $HX(q)$, first remove the edges connecting the second half of the second mirror copy. The vertices freed by this removal are then connected to half of the boundary vertices of the third copy. Subsequently, the remaining boundary vertices of the third copy are connected to the boundary vertices of the first copy, ensuring structural cohesion and continuity, as shown in Figure 5.

Step 4: This iterative process can be continued to construct a generalized hexagonal cage network HXC_p^q, consisting of p copies of $HX(q)$. The resulting structure is illustrated in Figure 6.

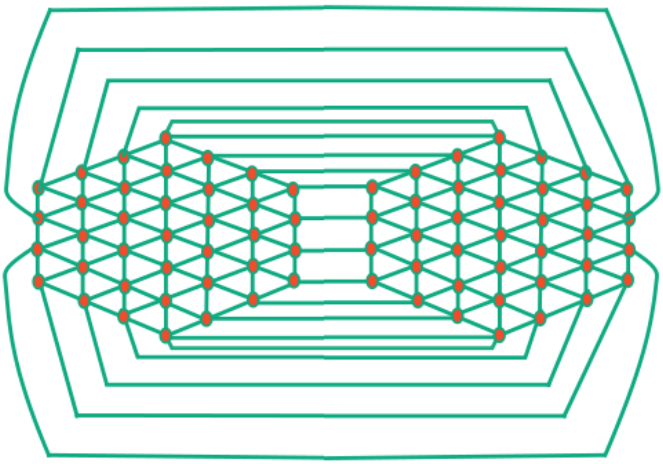

Figure 4. Generalized cage network formed by two mirrored copies of $HX(q)$.

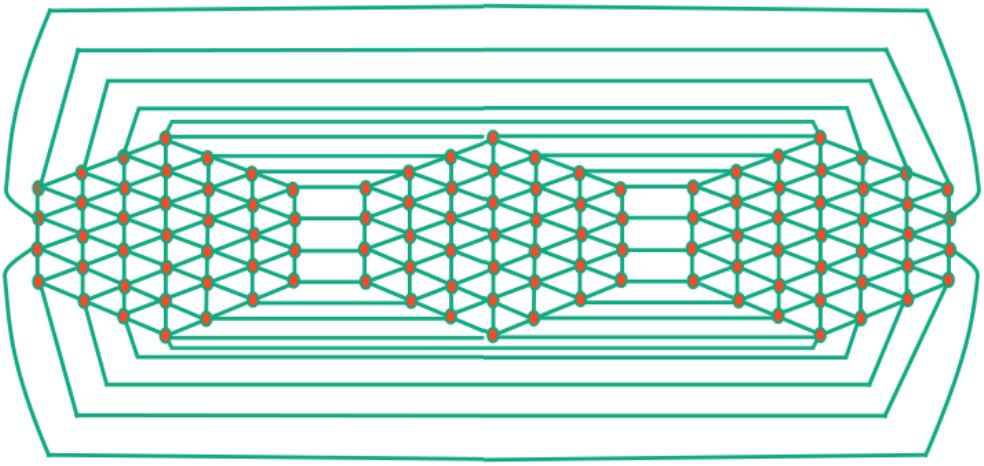

Figure 5. Hexagonal cage network with three copies, HXC_3^q.

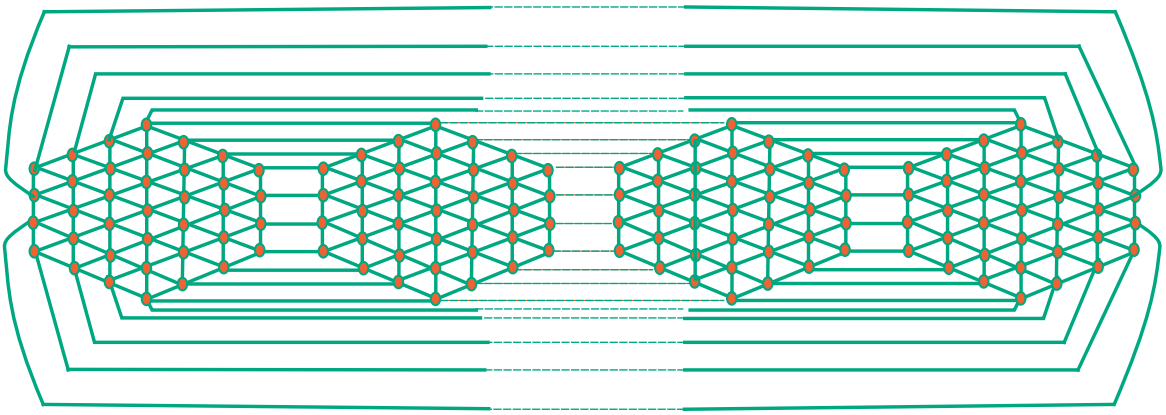

Figure 6. Generalized hexagonal cage network with p copies, HXC_p^q.

2.2. Edge partition of $S(HXC_p^q)$

The edge partition is derived from the structure of the generalized hexagonal cage network HXC_p^q. In HXC_p^q, the vertices have degrees 4, 5, and 6. During the subdivision process, every edge is replaced by a path of length two by inserting a new vertex of degree 2, while the degrees of the original vertices remain unchanged. Consequently, every edge in $S(HXC_p^q)$ joins a subdivision vertex of degree 2 with an original vertex of degree 4, 5, or 6. Therefore, the edge set naturally partitions into three disjoint classes according to the degrees of the end vertices.

Let $V(G)$ and $E(G)$ denote the vertex and edge sets of a graph G, respectively, and let $\deg(v)$ represent the degree of a vertex $v \in V(G)$. The edge classes of $S(HXC_p^q)$ are defined as

$$E_1(S(HXC_p^q)) = \{\, uv \in E(S(HXC_p^q)) : \deg(u) = 2,\ \deg(v) = 4 \,\},$$

$$E_2(S(HXC_p^q)) = \{\, uv \in E(S(HXC_p^q)) : \deg(u) = 2,\ \deg(v) = 5 \,\},$$

$$E_3(S(HXC_p^q)) = \{\, uv \in E(S(HXC_p^q)) : \deg(u) = 2,\ \deg(v) = 6 \,\}.$$

The cardinalities of these edge classes are obtained by direct counting from the structure of $S(HXC_p^q)$ and are summarized in Table 1.

Table 1. Edge partition of $S(HXC_p^q)$ according to the degrees of the end vertices.

Edge class	Degree pair $(\deg(u), \deg(v))$	Number of edges
E_1	$(2, 4)$	$20 + 4q$
E_2	$(2, 5)$	$-70 + 52p + 56q$
E_3	$(2, 6)$	$-30 + 40p + 40q$

Clearly,

$$E(S(HXC_p^q)) = E_1 \cup E_2 \cup E_3, \qquad E_i \cap E_j = \emptyset, \quad i \neq j.$$

The above edge partition serves as the foundation for computing all degree-based topological indices investigated in this paper.

Theorem 2.1. *Let $S(HXC_p^q)$ be the subdivided hexagonal cage network with p copies and order q. Then, the general Randić index*

$$R_\alpha(S(HXC_p^q)) = \sum_{uv \in E(S(HXC_p^q))} (d(u)d(v))^\alpha,$$

for $\alpha \in \left\{1, \frac{1}{2}, -\frac{1}{2}, -1\right\}$, is given by

$$R_\alpha(S(HXC_p^q)) = \begin{cases} -900 + 1000p + 1072q, & \alpha = 1, \\ -268.714 + 303.711p + 326.941q, & \alpha = \dfrac{1}{2}, \\ -23.73 + 28.00p + 30.67q, & \alpha = -\dfrac{1}{2}, \\ -7 + \dfrac{128}{15}p + \dfrac{283}{30}q, & \alpha = -1. \end{cases}$$

Proof. Using the edge partition of $S(HXC_p^q)$ given in Table 1, we compute the general Randić index for different values of α.

For $\alpha = 1$, we have

$$\begin{aligned} R_1(S(HXC_p^q)) &= \sum_{uv\in E(S(HXC_p^q))} d(u)d(v) \\ &= 8|E_1| + 10|E_2| + 12|E_3| \\ &= 8(20+4q) + 10(-70+52p+56q) + 12(-30+40p+40q) \\ &= 160 + 32q - 700 + 520p + 560q - 360 + 480p + 480q \\ &= -900 + 1000p + 1072q. \end{aligned}$$

For $\alpha = \dfrac{1}{2}$, we obtain

$$\begin{aligned} R_{\frac{1}{2}}(S(HXC_p^q)) &= \sum_{uv\in E(S(HXC_p^q))} (d(u)d(v))^{\frac{1}{2}} \\ &= \sqrt{8}\,|E_1| + \sqrt{10}\,|E_2| + \sqrt{12}\,|E_3| \\ &= \sqrt{8}(20+4q) + \sqrt{10}(-70+52p+56q) + \sqrt{12}(-30+40p+40q) \\ &= 40\sqrt{2} - 70\sqrt{10} - 60\sqrt{3} + \left(52\sqrt{10} + 80\sqrt{3}\right)p + \left(8\sqrt{2} + 56\sqrt{10} + 80\sqrt{3}\right)q \\ &\approx -268.714 + 303.711p + 326.941q. \end{aligned}$$

For $\alpha = -\dfrac{1}{2}$, we have

$$\begin{aligned} R_{-\frac{1}{2}}(S(HXC_p^q)) &= \sum_{uv\in E(S(HXC_p^q))} (d(u)d(v))^{-\frac{1}{2}} \\ &= \frac{1}{\sqrt{8}}|E_1| + \frac{1}{\sqrt{10}}|E_2| + \frac{1}{\sqrt{12}}|E_3| \\ &= \frac{1}{\sqrt{8}}(20+4q) + \frac{1}{\sqrt{10}}(-70+52p+56q) + \frac{1}{\sqrt{12}}(-30+40p+40q) \\ &\approx -23.73 + 28.00p + 30.67q. \end{aligned}$$

Finally, for $\alpha = -1$, we obtain

$$\begin{aligned} R_{-1}(S(HXC_p^q)) &= \sum_{uv\in E(S(HXC_p^q))} (d(u)d(v))^{-1} \\ &= \frac{1}{8}|E_1| + \frac{1}{10}|E_2| + \frac{1}{12}|E_3| \\ &= \frac{1}{8}(20+4q) + \frac{1}{10}(-70+52p+56q) + \frac{1}{12}(-30+40p+40q) \\ &= -7 + \frac{128}{15}p + \frac{283}{30}q. \end{aligned}$$

This completes the proof. □

Table 2 presents the values of $R_1(S(HXC_p^q))$, $R_{\frac{1}{2}}(S(HXC_p^q))$, $R_{-\frac{1}{2}}(S(HXC_p^q))$, and $R_{-1}(S(HXC_p^q))$ for the subdivided hexagonal cage networks with $p = q$ and $2 \leq p, q \leq 10$. Figure 7 illustrates the variation of these four Randić indices with respect to the parameter p.

Table 2. Randić topological indices of $S(HXC_p^q)$ for $2 \leq p, q \leq 10$ with $p = q$.

p	q	$R_1(S(HXC_p^q))$	$R_{\frac{1}{2}}(S(HXC_p^q))$	$R_{-\frac{1}{2}}(S(HXC_p^q))$	$R_{-1}(S(HXC_p^q))$
2	2	3244	992.590	93.61	28.9333
3	3	5316	1623.242	152.28	46.9000
4	4	7388	2253.894	210.95	64.8667
5	5	9460	2884.546	269.62	82.8333
6	6	11532	3515.198	328.29	100.8000
7	7	13604	4145.850	386.96	118.7667
8	8	15676	4776.502	445.63	136.7333
9	9	17748	5407.154	504.30	154.7000
10	10	19820	6037.806	562.97	172.6667

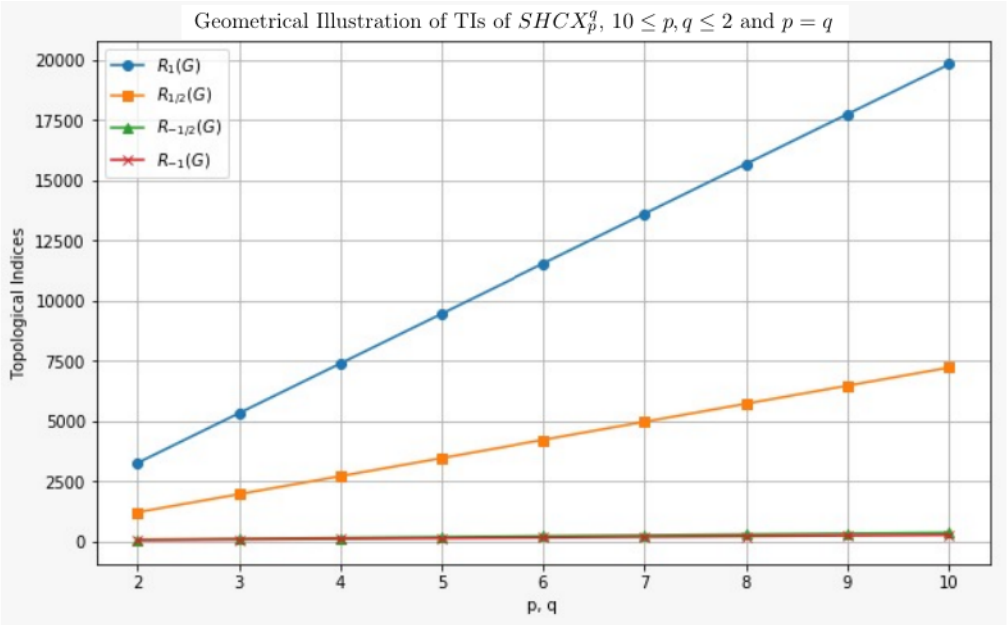

Figure 7. Graphical comparison of the Randić topological indices of $S(HXC_p^q)$ for $2 \leq p, q \leq 10$ with $p = q$. The plot illustrates the linear growth trends of the R_1, $R_{\frac{1}{2}}$, $R_{-\frac{1}{2}}$, and R_{-1} indices as the network size increases.

- The x-axis represents the parameter p.
- The y-axis represents the corresponding Randić index value.
- Four distinct curves corresponding to $\mathbf{R_1}$, $\mathbf{R_{1/2}}$, $\mathbf{R_{-1/2}}$, and $\mathbf{R_{-1}}$ are plotted with markers indicating the computed values.
- The curve of $\mathbf{R_1}$ exhibits the largest magnitude and the steepest linear growth, followed by $\mathbf{R_{1/2}}$, $\mathbf{R_{-1/2}}$, and $\mathbf{R_{-1}}$.

- The plot includes descriptive axis labels, a legend, and the title *"Randić Indices of $S(HXC_p^q)$ for $p = q$"*, as shown in Figure 7.

Theorem 2.2. *Let $S(HXC_p^q)$ be the subdivided hexagonal cage network with p copies and order q. Then, the Zagreb indices of $S(HXC_p^q)$ are given by*

$$M_i(S(HXC_p^q)) = \begin{cases} -610 + 684p + 736q, & i = 1, \\ -900 + 1000p + 1072q, & i = 2, \\ -290 + 316p + 336q, & i = 3. \end{cases}$$

Proof. Using the edge partition of $S(HXC_p^q)$ given in Table 1, we compute the three Zagreb indices as follows.

For the first Zagreb index,

$$\begin{aligned} M_1(S(HXC_p^q)) &= \sum_{uv \in E(S(HXC_p^q))} [d(u) + d(v)] \\ &= 6|E_1| + 7|E_2| + 8|E_3| \\ &= 6(20 + 4q) + 7(-70 + 52p + 56q) + 8(-30 + 40p + 40q) \\ &= 120 + 24q - 490 + 364p + 392q - 240 + 320p + 320q \\ &= -610 + 684p + 736q. \end{aligned}$$

For the second Zagreb index,

$$\begin{aligned} M_2(S(HXC_p^q)) &= \sum_{uv \in E(S(HXC_p^q))} d(u)d(v) \\ &= 8|E_1| + 10|E_2| + 12|E_3| \\ &= 8(20 + 4q) + 10(-70 + 52p + 56q) + 12(-30 + 40p + 40q) \\ &= 160 + 32q - 700 + 520p + 560q - 360 + 480p + 480q \\ &= -900 + 1000p + 1072q. \end{aligned}$$

Finally, for the third Zagreb index,

$$\begin{aligned} M_3(S(HXC_p^q)) &= \sum_{uv \in E(S(HXC_p^q))} |d(u) - d(v)| \\ &= 2|E_1| + 3|E_2| + 4|E_3| \\ &= 2(20 + 4q) + 3(-70 + 52p + 56q) + 4(-30 + 40p + 40q) \\ &= 40 + 8q - 210 + 156p + 168q - 120 + 160p + 160q \\ &= -290 + 316p + 336q. \end{aligned}$$

Hence,

$$M_i(S(HXC_p^q)) = \begin{cases} -610 + 684p + 736q, & i = 1, \\ -900 + 1000p + 1072q, & i = 2, \\ -290 + 316p + 336q, & i = 3. \end{cases}$$

This completes the proof. □

Theorem 2.3. *Let $S(HXC_p^q)$ be the subdivided hexagonal cage network with p copies and order q. Then, the geometric–arithmetic (GA) index of $S(HXC_p^q)$ is given by*

$$GA(S(HXC_p^q)) = \left(\frac{40\sqrt{2}}{3} - 20\sqrt{10} - 15\sqrt{3}\right) + \left(\frac{104\sqrt{10}}{7} + 20\sqrt{3}\right)p + \left(\frac{8\sqrt{2}}{3} + 16\sqrt{10} + 20\sqrt{3}\right)q.$$

Proof. Using the edge partition of $S(HXC_p^q)$ given in Table 1, the geometric–arithmetic (GA) index is

$$GA(S(HXC_p^q)) = \sum_{uv \in E(S(HXC_p^q))} \frac{2\sqrt{d(u)d(v)}}{d(u)+d(v)}.$$

Therefore,

$$\begin{aligned} GA(S(HXC_p^q)) &= \frac{2\sqrt{2}}{3}|E_1| + \frac{2\sqrt{10}}{7}|E_2| + \frac{\sqrt{3}}{2}|E_3| \\ &= \frac{2\sqrt{2}}{3}(20+4q) + \frac{2\sqrt{10}}{7}(-70+52p+56q) + \frac{\sqrt{3}}{2}(-30+40p+40q) \\ &= \left(\frac{40\sqrt{2}}{3} - 20\sqrt{10} - 15\sqrt{3}\right) + \left(\frac{104\sqrt{10}}{7} + 20\sqrt{3}\right)p \\ &\quad + \left(\frac{8\sqrt{2}}{3} + 16\sqrt{10} + 20\sqrt{3}\right)q. \end{aligned}$$

This completes the proof. □

Finally, we derive the ABC index, which is one of the most important degree-based topological indices for the subdivided hexagonal cage network.

Theorem 2.4. *Let $S(HXC_p^q)$ be the subdivided hexagonal cage network with p copies and order q. Then, the ABC index of $S(HXC_p^q)$ is given by*

$$ABC(S(HXC_p^q)) = 46\sqrt{2}\,p + 50\sqrt{2}\,q - 40\sqrt{2}.$$

Equivalently,

$$ABC(S(HXC_p^q)) = \frac{92p + 100q - 80}{\sqrt{2}}.$$

Proof. Using the edge partition of $S(HXC_p^q)$ given in Table 1, the ABC index is

$$ABC(S(HXC_p^q)) = \sum_{uv \in E(S(HXC_p^q))} \sqrt{\frac{d(u)+d(v)-2}{d(u)d(v)}}.$$

Therefore,

$$\begin{aligned} ABC(S(HXC_p^q)) &= \sqrt{\frac{2+4-2}{2\cdot 4}}\,|E_1| + \sqrt{\frac{2+5-2}{2\cdot 5}}\,|E_2| + \sqrt{\frac{2+6-2}{2\cdot 6}}\,|E_3| \\ &= \sqrt{\frac{1}{2}}(20+4q) + \sqrt{\frac{1}{2}}(-70+52p+56q) + \sqrt{\frac{1}{2}}(-30+40p+40q) \\ &= \frac{1}{\sqrt{2}}\left[(20+4q)+(-70+52p+56q)+(-30+40p+40q)\right] \\ &= \frac{92p+100q-80}{\sqrt{2}} \\ &= 46\sqrt{2}\,p + 50\sqrt{2}\,q - 40\sqrt{2}. \end{aligned}$$

This completes the proof. □

Theorem 2.5. *Let $S(HXC_p^q)$ be the subdivided hexagonal cage network with p copies and order q. Then, the hyper-Zagreb index of $S(HXC_p^q)$ is given by*

$$HM(S(HXC_p^q)) = -4630 + 5108p + 5448q.$$

Proof. Using the edge partition of $S(HXC_p^q)$ given in Table 1, the hyper-Zagreb index is

$$HM(S(HXC_p^q)) = \sum_{uv\in E(S(HXC_p^q))} (d(u)+d(v))^2.$$

Therefore,

$$\begin{aligned} HM(S(HXC_p^q)) &= 36|E_1| + 49|E_2| + 64|E_3| \\ &= 36(20+4q) + 49(-70+52p+56q) + 64(-30+40p+40q) \\ &= 720 + 144q - 3430 + 2548p + 2744q - 1920 + 2560p + 2560q \\ &= -4630 + 5108p + 5448q. \end{aligned}$$

This completes the proof. □

3. Numerical and graphical representation

Computed topological indices of the subdivided hexagonal cage network $S(HXC_p^q)$ for $p, q \geq 2$ with $p = q$. The table lists the first, second, and third Zagreb indices (M_1, M_2, M_3), the geometric index (GA), atom-bond connectivity index (ABC), and hyper-Zagreb index (HM) for different network orders. Table 3 presents detailed information on $S(HXC_p^q)$, providing insights into structure–activity correlations and molecular characteristics for $2 \leq p, q \leq 10$ with $p = q$.

The graph clearly illustrates the following trends as the parameter p increases from 2 to 10 in Figure 8.

- The index HM exhibits the steepest growth and consistently has the largest values across the entire range of p.

- The indices M_1 and M_2 grow at a comparable and moderately fast rate, maintaining their position significantly above M_3, GA, and ABC, but well below HM. Moreover, M_2 is consistently higher than M_1.
- The indices M_3, GA, and ABC form the lowest-valued group. Their values are clustered together, though they also show a distinct increasing trend. Among these, M_3 generally has the highest values, followed closely by GA and then ABC.
- All six metrics show a monotonically increasing trend with respect to the parameter p, suggesting a polynomial or exponential relationship between p and the metric values.

For $p = 3$ and $q = 3$, the second Zagreb index (M_2) is calculated to be 13,420. Higher values of M_2 are often associated with physical properties such as molecular weight and boiling point. This index reflects a more-complex network with stronger connectivity, which may affect the compound's stability, see Figure 9.

For $p = 5$ and $q = 5$, the third Zagreb index (M_3) is 5994. This index provides insights into the stability and reactivity of the hexagonal cage network, offering a deeper understanding of the molecular structure, see Figure 10.

Finally, for $p = 7$ and $q = 7$, the hyper-Zagreb index (HM) is 409,264. A higher HM value indicates a more complex chemical structure, which can significantly impact the stability and reactivity of the hexagonal cage network.

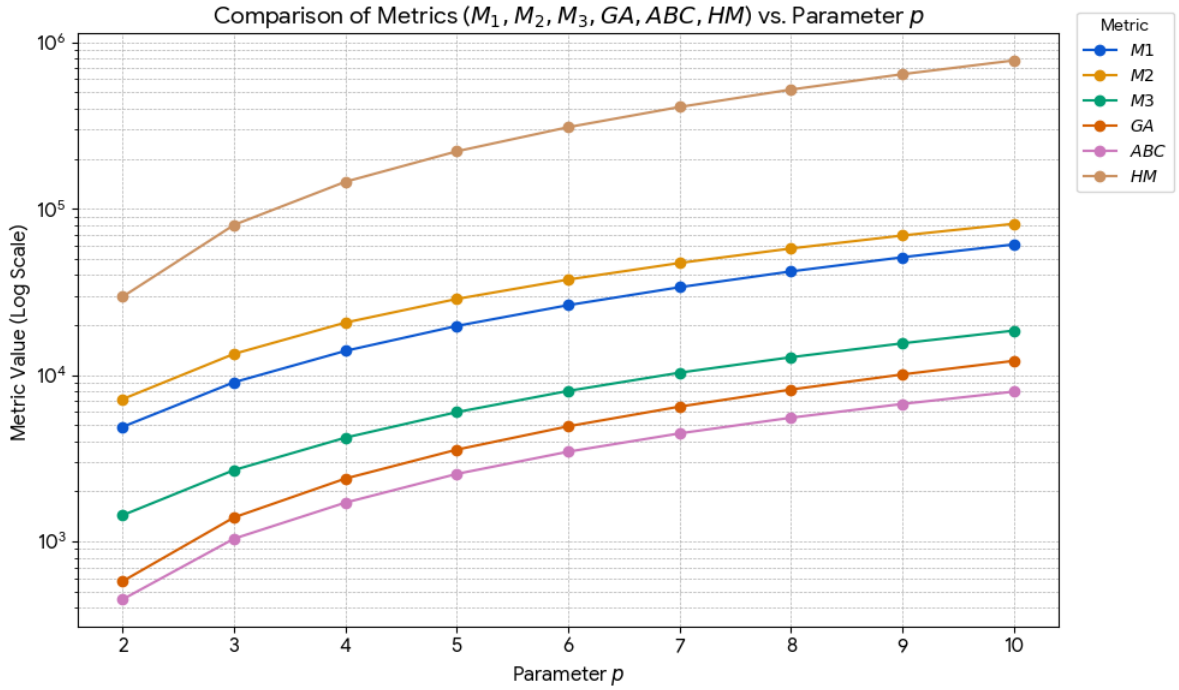

Figure 8. Graphical comparison among topological indices of $S(HXC_p^q)$.

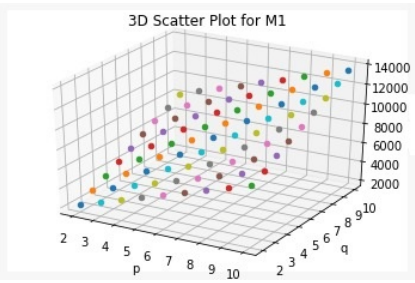

(**a**) First Zagreb index

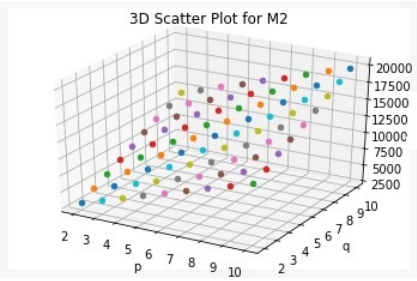

(**b**) Second Zagreb index

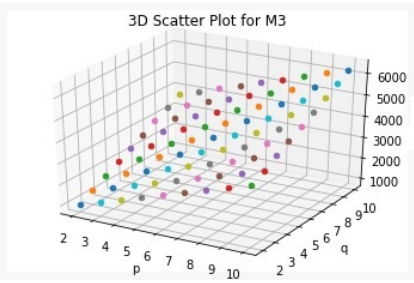

(**c**) Third Zagreb index

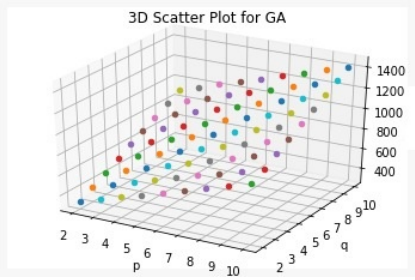

(**d**) Geometric index

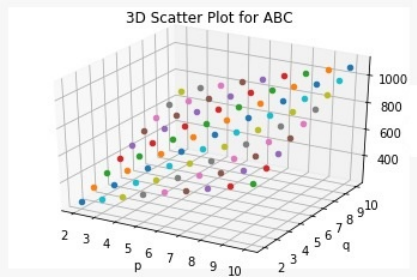

(**e**) Atom-bond connectivity index

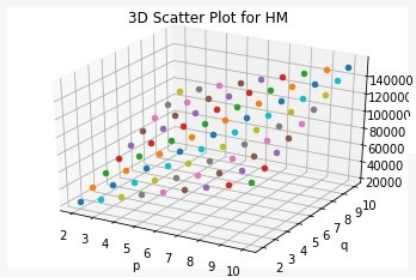

(**f**) Hyper Zagreb index

Figure 9. Topological indices and molecular descriptors for the hexagonal cage network, graphical scatered diagram.

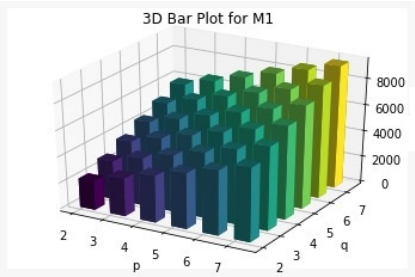

(a) First Zagreb index

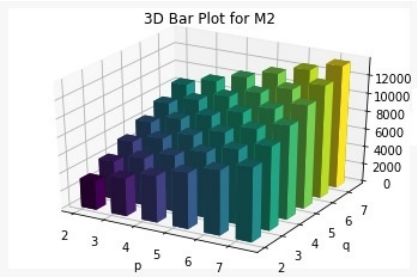

(b) Second Zagreb index

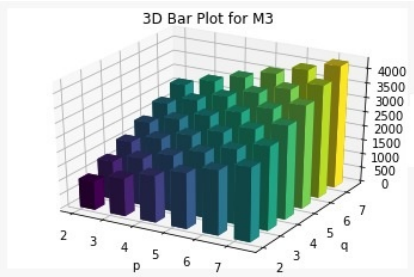

(c) Third Zagreb index

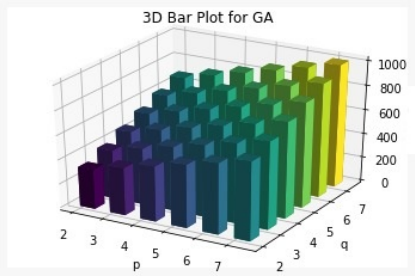

(d) Geometric index

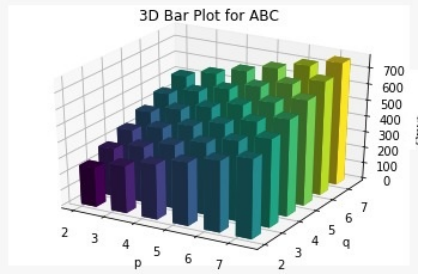

(e) Atom-bond connectivity index

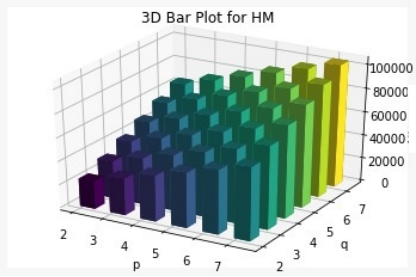

(f) Hyper Zagreb index

Figure 10. Comparison of topological indices and molecular descriptors for the hexagonal cage network, graphical bar diagram.

Table 3. Computed values of the degree-based topological indices of $S(HXC_p^q)$ for $2 \leq p, q \leq 10$ with $p = q$.

p	q	M_1	M_2	M_3	GA	ABC	HM
2	2	2230	3244	1014	576.6756	448.7289	29584
3	3	3650	5316	1666	1346.5856	1039.7087	79960
4	4	5070	7388	2318	2116.4956	1713.0076	145336
5	5	6490	9460	2970	2886.4056	2548.6256	221512
6	6	7910	11532	3622	3656.3156	3466.5627	309488
7	7	9330	13604	4274	4426.2256	4466.8189	409264
8	8	10750	15676	4926	5196.1356	5549.3942	520840
9	9	12170	17748	5578	5966.0456	6714.2886	644216
10	10	13590	19820	6230	6735.9556	7961.5021	779392

4. Applications and graphical illustration

To further highlight the practical relevance of the obtained results, we present a graphical illustration summarizing the key structural and analytical insights of the proposed model. Figure 11 provides a visual interpretation of the theoretical framework developed in this study and helps in understanding the relationship between graph-theoretical parameters and their corresponding chemical and material properties. Such visual representation bridges the gap between mathematical formulation and real-world applicability.

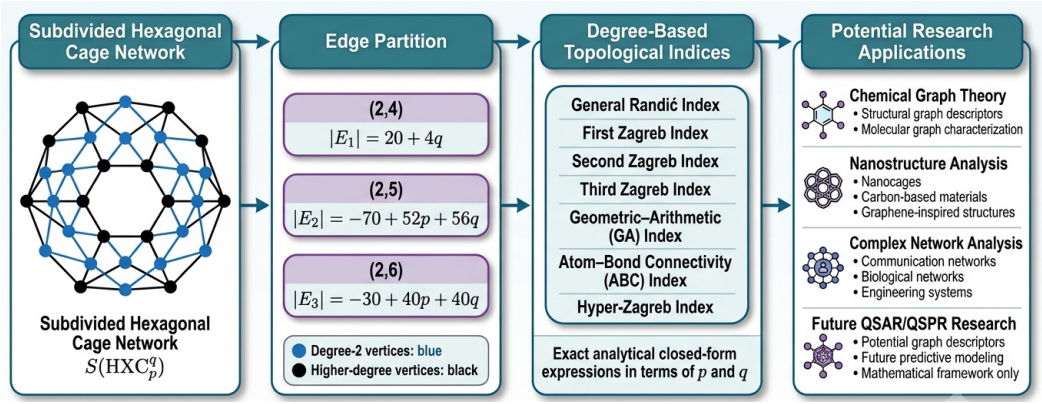

Figure 11. Applications and graphical illustration of indices.

The proposed topological framework is highly significant in the context of chemical graph theory and material science. In particular, the derived indices and structural descriptors can be effectively utilized in quantitative structure–property relationship (QSPR) and quantitative structure–activity relationship (QSAR) studies. These results are useful in modeling molecular stability, predicting physicochemical properties, and designing novel materials with desired characteristics. The schematic diagram in the figure encapsulates these applications in a compact and intuitive form.

5. Conclusions

In this research, we studied the subdivision of the hexagonal cage network of order P with Q copies by adding a new vertex on each edge, resulting in a subdivided network of order q with p copies. A class of degree-based topological indices—including the general Randić index, first, second, and third Zagreb indices; and atom-bond connectivity indices—was analyzed both statistically and computationally. The study demonstrates that examining these indices provides valuable insights into the structure-activity relationships and molecular characteristics of the network. These findings have potential implications in fields such as toxicology, pharmacology, and materials science, potentially guiding the design of safer pharmaceuticals and novel materials. Further research should explore molecular descriptors derived from other network constructions, such as corona and modular products, to enhance the precision of molecular characterization. Overall, the study of topological indices in relation to molecular structures holds significant promise for advancing materials science and drug development, offering deeper understanding of molecular properties and guiding rational design strategies.

Author contributions

Muhammad Abdullah: Conceptualization, Methodology, Formal analysis, Investigation, Validation, Writing–original draft. **Muhammad Usman Ghani:** Conceptualization, Supervision, Methodology, Validation, Writing–review and editing, Project administration, Correspondence. **Hanen Karamti:** Formal analysis, Validation, Writing–review and editing. **Syed Ajaz K. Kirmani:** Investigation, Validation, Writing–review and editing. All authors have read and agreed to the published version of the manuscript.

Use of Generative-AI tools declaration

The authors declare that no generative Artificial Intelligence (AI) tools were used in the preparation of this manuscript.

Acknowledgments

The work was supported by the Princess Nourah bint Abdulrahman University Researchers Supporting Project number (PNURSP2026R192), Princess Nourah bint Abdulrahman University, Riyadh, Saudi Arabia.

Conflict of interest

The authors declare no conflicts of interest.

References

1. J. B. Liu, K. Wang, X. Zhai, Statistical analysis and topological property of a class of fractal networks, *Fractals*, **34** (2026), 2640001. https://doi.org/10.1142/S0218348X26400013

2. M. U. Ghani, S. Ali, M. Imran, H. Karamti, F. Sultan, M. Y. Almusawa, Hex-derived molecular descriptors via generalized valency-based entropies, *IEEE Access*, **11** (2023), 42052–42068. https://doi.org/10.1109/ACCESS.2023.3248507

3. K. M. Siddique, K. Julietraja, P. Venugopal, S. Deepa, Molecular structural descriptors of donut benzenoid systems, *Polycycl. Aromat. Comp.*, **42** (2022), 4146–4172. https://doi.org/10.1080/10406638.2021.1885456

4. M. Imran, A. R. Khan, M. N. Husin, F. Tchier, M. U. Ghani, S. Hussain, Computation of entropy measures for metal–organic frameworks, *Molecules*, **28** (2023), 4726. https://doi.org/10.3390/molecules28124726

5. G. F. Yu, M. K. Siddiqui, M. Hussain, N. Hussain, Topological invariants of sustainable network for energy efficiency, *Chaos Soliton. Fract.*, **208** (2026), 118060. https://doi.org/10.1016/j.chaos.2026.118060

6. M. U. Ghani, F. J. H. Campena, M. K. Maqbool, J. B. Liu, S. Dehraj, M. Cancan, et al., Entropy related to K-Banhatti indices via valency based on the presence of C_6H_6 in various molecules, *Molecules*, **28** (2023), 452. https://doi.org/10.3390/molecules28010452

7. D. A. Xavier, A. Theertha Nair, M. U. Ghani, A. Baby, F. Tchier, Computing molecular descriptors of boron icosahedral sheet, *Int. J. Quantum Chem.*, **124** (2024), e27443. https://doi.org/10.1002/qua.27443

8. J. B. Liu, F. Zou, G. J. Cai, J. Cao, Network coherence and robustness analysis of extended polygonal networks, *Circuits Syst. Signal Process.*, 2026. https://doi.org/10.1007/s00034-026-03526-1

9. M. Arockiaraj, J. B. Liu, M. Arulperumjothi, S. Prabhu, On certain topological indices of three-layered single-walled titania nanosheets, *Comb. Chem. High T. Scr.*, **25** (2022), 483–495. https://doi.org/10.2174/1386207323666201012143430

10. M. U. Ghani, M. Imran, S. Sampathkumar, F. Tchier, K. Pattabiraman, A. Z. Jan, A paradigmatic approach to the molecular descriptor computation for some antiviral drugs, *Heliyon*, **9** (2023), e19957. https://doi.org/10.1016/j.heliyon.2023.e19957

11. J. Zhang, Z. Liu, B. Zhou, On the maximal eccentric connectivity indices of graphs, *Appl. Math. J. Chinese Univ.*, **29** (2014), 374–378. https://doi.org/10.1007/s11766-014-3023-7

12. J. B. Liu, X. J. Tang, G. J. Cai, J. Cao, Spectrum and coherence analysis in networks with noise disturbance, *J. Complex Netw.*, **14** (2026), cnaf046. https://doi.org/10.1093/comnet/cnaf046

13. M. Arockiaraj, S. Prabhu, M. Arulperumjothi, S. Kavitha, K. Balasubramanian, Topological characterization of hexagonal and rectangular tessellations of kekulenes as traps for toxic heavy metal ions, *Theor. Chem. Acc.*, **140** (2021), 43. https://doi.org/10.1007/s00214-021-02733-0

14. M. Radhakrishnan, S. Prabhu, M. Arockiaraj, M. Arulperumjothi, Molecular structural characterization of superphenalene and supertriphenylene, *Int. J. Quantum Chem.*, **122** (2022), e26818. https://doi.org/10.1002/qua.26818

15. I. Gutman, N. Trinajstić, Graph theory and molecular orbitals: total π-electron energy of alternant hydrocarbons, *Chem. Phys. Lett.*, **17** (1972), 535–538. https://doi.org/10.1016/0009-2614(72)85099-1

16. C. C. Wei, M. Salman, U. Ali, M. U. Rehman, M. A. Ahmad Khan, M. H. Chaudary, et al., Some topological invariants of graphs associated with the group of symmetries, *J. Chem.*, **2020** (2020), 6289518. https://doi.org/10.1155/2020/6289518

17. F. Ali, M. Salman, A. Hafeez, S. Huang, On computation of some distance-based topological indices on circulant networks-II, *J. Inf. Optim. Sci.*, **39** (2018), 759–782. https://doi.org/10.1080/02522667.2016.1223588

18. L. Zhang, T. L. Sun, M. Arockiaraj, M. Arulperumjothi, S. Prabhu, Wiener polarity index calculation of square-free graphs and its implementation to certain complex materials, *Math. Probl. Eng.*, **2021** (2021), 6686352. https://doi.org/10.1155/2021/6686352

19. F. Ali, M. Salman, S. Huang, On the commuting graph of dihedral group, *Commun. Algebra*, **44** (2016), 2389–2401. https://doi.org/10.1080/00927872.2015.1039770

20. A. S. Alali, S. Ali, N. Hassan, A. M. Mahnashi, Y. Shang, A. Assiry, Algebraic structure graphs over the commutative ring $\mathbb{Z}_m$: exploring topological indices and entropies using M-polynomials, *Mathematics*, **11** (2023), 3833. https://doi.org/10.3390/math11183833

21. A. R. Ashrafi, A. Ghalavand, Ordering chemical trees by Wiener polarity index, *Appl. Math. Comput.*, **313** (2017), 301–312. https://doi.org/10.1016/j.amc.2017.06.005

22. H. Hua, K. Das, On the Wiener polarity index of graphs, *Appl. Math. Comput.*, **280** (2016), 162–167. https://doi.org/10.1016/j.amc.2016.01.043

23. L. Chen, T. Li, Y. Shi, H. Wang, On the Wiener polarity index of lattice networks, *PLOS ONE*, **11** (2016), e0167075. https://doi.org/10.1371/journal.pone.0167075

24. A. Ilić, M. Ilić, Generalizations of Wiener polarity index and terminal Wiener index, *Graphs Comb.*, **29** (2013), 1403–1416. https://doi.org/10.1007/s00373-012-1215-6

25. M. A. Awan, S. Ali, N. Hassan, Y. Shang, A. M. Mahnashi, A. Assiry, Several characterizations on degree-based topological indices for star of David network, *Numer. Methods Partial Differential Equations*, **39** (2023), 3743–3761. https://doi.org/10.1002/num.23027

26. M. Randić, Characterization of molecular branching, *J. Amer. Chem. Soc.*, **97** (1975), 6609–6615. https://doi.org/10.1021/ja00856a001

27. Y. Zhang, Y. Zhang, G. Li, J. Lu, X. Lin, Y. Tan, et al., Construction of single-crystalline supramolecular networks of perchlorinated hexa-peri-hexabenzocoronene on Au(111), *J. Chem. Phys.*, **142** (2015), 101911. https://doi.org/10.1063/1.4914301

28. E. Estrada, L. Torres, L. Rodriguez, I. Gutman, An atom-bond connectivity index: modelling the enthalpy of formation of alkanes, *Indian J. Chem. Sect. A*, **37** (1998), 849–855.

29. Y. Z. Tan, B. Yang, K. Parvez, A. Narita, S. Osella, D. Beljonne, et al., Atomically precise edge chlorination of nanographenes and its application in graphene nanoribbons, *Nat. Commun.*, **4** (2013), 2646. https://doi.org/10.1038/ncomms3646

30. L. Chen, Y. Hernandez, X. Feng, K. Müllen, From nanographene and graphene nanoribbons to graphene sheets: Chemical synthesis, *Angew. Chem. Int. Ed.*, **51** (2012), 7640–7654. https://doi.org/10.1002/anie.201201084

31. X. Shi, S. Kosari, U. Ahmad, S. Hameed, S. Akhter, Evaluation of various topological indices of Flabellum graphs, *Mathematics*, **11** (2023), 4167. https://doi.org/10.3390/math11194167

32. S. Lal, V. Kumar Bhat, K. Sharma, S. Sharma, Topological indices of lead sulphide using polynomial technique, *Mol. Phys.*, **122** (2024), e2249131. https://doi.org/10.1080/00268976.2023.2249131

33. K. Sharma, V. K. Bhat, J. B. Liu, Second leap hyper-Zagreb coindex of certain benzenoid structures and their polynomials, *Comput. Theor. Chem.*, **1223** (2023), 114088. https://doi.org/10.1016/j.comptc.2023.114088

34. S. Lal, V. K. Bhat, S. Sharma, Topological indices and graph entropies for carbon nanotube Y-junctions, *J. Math. Chem.*, **62** (2024), 73–108. https://doi.org/10.1007/s10910-023-01588-3

35. S. Sharma, V. K. Bhat, S. Lal, The metric resolvability and topological characterisation of some molecules in H1N1 antiviral drugs, *Mol. Simulat.*, **49** (2023), 1165–1178. https://doi.org/10.1080/08927022.2023.2223718

36. M. U. Ghani, F. Sultan, E. S. M. Tag El Din, A. R. Khan, J. B. Liu, M. Cancan, A paradigmatic approach to find the valency-based K-Banhatti and redefined Zagreb entropy for niobium oxide and a metal–organic framework, *Molecules*, **27** (2022), 6975. https://doi.org/10.3390/molecules27206975

AIMS Press